Melting of the Martian mantle from 1.0 to 4.5 GPa

Kyoko N. MATSUKAGE[*,‡], Yoko NAGAYO[*,†], Matthew L. WHITAKER[*,§], Eiichi TAKAHASHI[**] and Toshisuke KAWASAKI[***]

[*]*Geodynamics Research Center, Ehime University, 2-5 Bunkyo-cho, Matsuyama, Ehime 790-8577, Japan*
[**]*Earth and Planetary Sciences, Tokyo Institute of Technology, 2-12-1 Ookayama, Meguro-ku, Tokyo 152-8551, Japan*
[***]*Earth Sciences, Ehime University, 2-5 Bunkyo-cho, Matsuyama, Ehime 790-8577, Japan*
[‡]*Present address: Graduate School of Human and Environmental Sciences, Kyoto University, Yoshida-Nihonmatsu-cho, Sakyo-ku, Kyoto 606-8501, Japan*
[†]*Present address: Kyushu University, 6-10-1 Hakozaki, Higashi-ku, Fukuoka 812-8581, Japan*
[§]*Present address: Mineral Physics Institute, Stony Brook University,Stony Brook, NY 11794-2100, USA*

To investigate the chemical composition of possible primitive melts of the Martian mantle, we performed melting experiments of a model Martian mantle derived by Dreibus and Wänke (DWM) at pressures from 1.0 to 4.5 GPa. The chemical compositions of partial melts are systematically related to pressure. The partial melts at pressure of 1.0 GPa in spinel stability field show high Al_2O_3 and low FeO contents. The partial melts at higher pressure in garnet stability field are, however, characterized by a relatively high FeO content, low Al_2O_3 content and high CaO/Al_2O_3 ratio. In garnet stability field, clinopyroxene (= Ca-rich phase) contribute significantly to melt formation near the solidus temperature, although garnet (= Al-rich phase) is stable at temperature above solidus. Therefore Al-poor and Ca-rich partial melt are formed at higher pressure. Comparing the shergottite chemistry with the chemical trends of the partial melts obtained by the experiments, we suggest that one of basaltic shergottite with a high Al_2O_3 and low CaO/Al_2O_3 ratio, QUE94201, resembles the composition of the DWM partial melts in major-element chemistry in a low degree (<20%) partial melt of DWM at pressure of 1.0 GPa and temperature of 1360 °C. We conclude that the olivine-poor (or olivine-free) basaltic magma with low CaO/Al_2O_3 ratio and high Al_2O_3 could be primitive melts derived from the upper mantle of Mars if the actual Martian mantle is similar in composition to DWM.

Keywords: Martian mantle, Martian basalt, Melting experiment, Shergottite

INTRODUCTION

The structure and chemical composition of the Martian interior have been constrained by both geophysical (moment of inertia, average density), and geochemical data (shergotteite, nakhlite and chassigny (SNC) meteorites, Martian soil and basalts) (e.g., Longhi et al., 1992). The SNC meteorites provide a strong constraint for the chemical composition of the Martian interior because they are igneous rocks considered to have originated from Mars (e.g., Pepin, 1985; Grimm and McSween, 1982). These meteorites are divided into distinct classes; shergottites, nakhlites, chassignites, and ALH84001. Shergottites are of particular use in estimating the chemical composition of the Martian mantle because they contain both cumulate and basaltic rocks, while the other three sets of Martian meteorites are only cumulate rocks. The basaltic shergottites vary significantly in chemistry and petrology, and are classified according to mineral assemblages into two subgroups; of olivine-phyric and olivine-free basalts (Goodrich, 2002). The olivine-phyric shergottite is characterized by the presence of large olivine crystals in a fine-grained groundmass. The olivine-free shergottite consists of pyroxenes and plagioclase with basaltic or diabasic textures.

Of the sub-groups within shergottites, the olivine-phyric shergottites are considered to be the most primitive (e.g., Zipfel et al., 2000; Irving et al., 2002, 2010b; Goodrich, 2003) and thus present the best opportunity to investigate possible Martian parental liquid compositions. However, several researchers (e.g., McSween and Jarosewich, 1983; Wadhwa et al., 2001; Barrat et al., 2002; Filiberto et al., 2010) have interpreted the olivine megacrysts

doi:10.2465/jmps.120820
K.N. Matsukage, matsukage.kyoko.8c@kyoto-u.ac.jp Corresponding author

Advance Publication Article

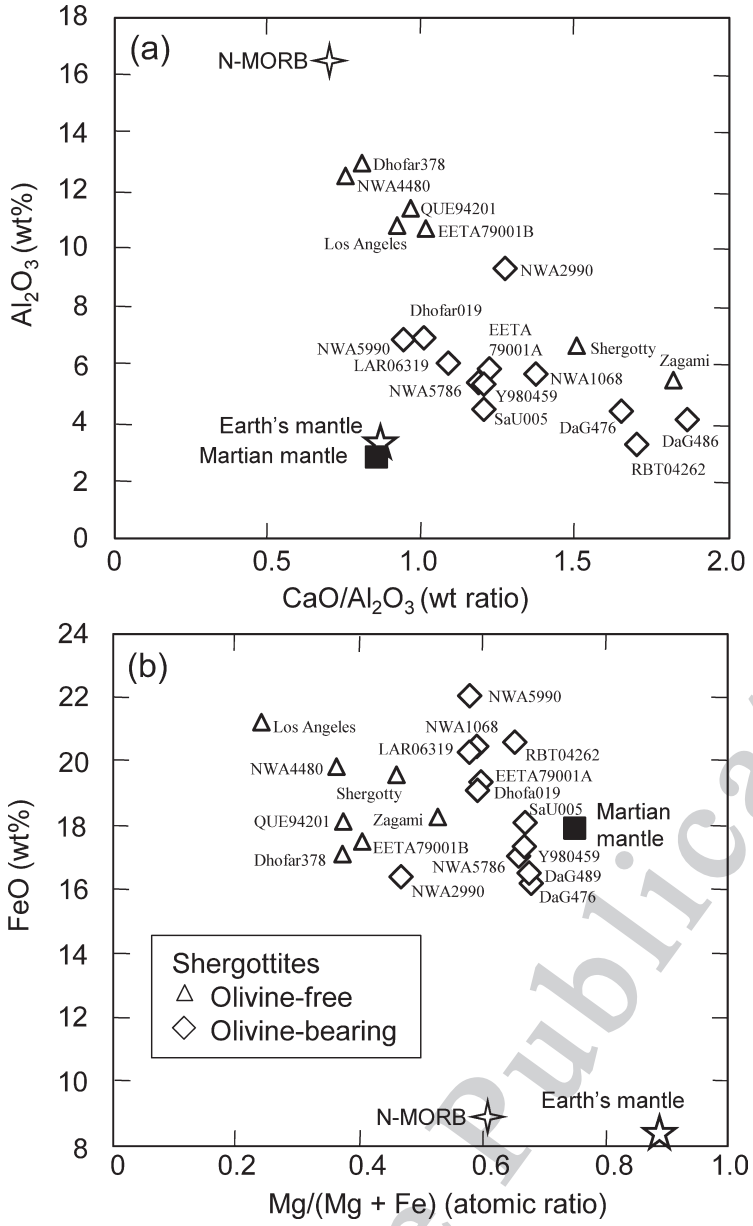

Figure 1. Chemical compositions of olivine-free and olivine-phyric basaltic shergottites, Martian mantle (DWM), pyrolite and N-MORB. Data for shergottites are after Zipfel et al. (2000), Barrat et al. (2001), Folco et al. (2000), Taylor et al. (2002), Dreibus et al. (2002), Ikeda et al. (2006), Meyer (2003), Rubin et al. (2000), Barrat et al. (2002), Gross et al. (2010), Irving et al. (2010a), Irving et al. (2010b), Dreibus et al. (1996), Warren et al. (1999), Kring et al. (2003), Anand et al. (2008), Dreibus et al. (2000), McCarthy et al. (1974), Stolper and McSween (1979), Dreibus et al. (1982), Barret et al. (2001), Misawa (2004), Easton and Elliot (1977), Stolper and McSween (1979), McCoy et al. (1991), Haramura (1995), Kong et al. (1999), Barrat et al. (2001), BasuSarbadhikari et al. (2009) and Bunch et al. (2009). Data for Martian mantle, pyrolite, and N-MORB are after Dreibus and Wänke (1985), Ringwood (1966), and Schilling et al. (1983), respectively.

in some olivine-phyric shergottites as exotic xenocrysts or cognate xenocrysts mixed into the olivine-free (or olivine-poor) basaltic magma by other processes. Despite the considerable number of studies conducted regarding the igneous origin of basaltic shergottites, the primitive (parent) magma composition of the Martian mantle remains controversial (e.g., Goodrich, 2002; Greshake et al., 2004; Shearer et al., 2008; Usui et al., 2008; Sarbadhikari et al., 2009; Peslier et al., 2010; Filiberto and Dasgupta, 2011).

Martian basaltic rocks are enriched in FeO component and depleted in Al_2O_3 (Fig. 1) relative to terrestrial basalts. On the basis of chemical compositions of Martian basaltic meteorites and chondritic meteorites, Dreibus and Wänke (1985) derived a Martian mantle composition, referred to as DWM in this work, which is also enriched in iron compared with Earth's mantle (Table. 1). For many years, the DWM has been considered to be one of most common model Martian mantle compositions (e.g., Bertka and Holloway, 1994; Bertka and Fei, 1997). To evaluate the 'parent-child relationship' between DWM and basaltic shergottites, Bertka and Holloway (1994a, 1994b) performed partial melting experiments by using the DWM composition at 1.5 GPa, and Agee and Draper (2004) performed melting experiments on the Homestead L5 ordinary chondrite at 5.0 GPa, which has similar composition as that of DWM. The compositions of low-degree melts at 1.5 GPa studied by Bertka and Holloway (1994b) were more enriched in Al than the shergottites parent melt (e.g., Stolper and McSween, 1979; McCoy et al., 1991; Hale et al., 1999). At 5 GPa, the low-degree melt produced by

Advance Publication Article

Table 1. Chemical compositions of model Earth (pyrolite), and Martian (DWM) mantles, and experimental starting material

(wt%)	Pyrolite[c]	DW Mars[d]	Starting material
SiO_2	45.2	44.4	44.7
TiO_2	0.7	0.1	0.1
Al_2O_3	3.5	2.9	3.0
Cr_2O_3	0.4	0.8	0.8
FeO*	8.5	17.9	18.0
MnO	0.1	0.46	
MgO	37.5	30.1	30.4
CaO	3.1	2.5	2.5
Na_2O	0.6	0.5	0.5
K_2O	0.1	0.04	
P_2O_5	0.1	0.17	
Total	99.8	99.8	100.0
Mg#[a]	0.887	0.750	0.750
CaO/Al_2O_3[b]	0.87	0.84	0.81

[a] Mg/(Mg + Fe) atomic ratio.
[b] wt ratio.
[c] After Ringwood (1966).
[d] Martian model mantle by Dreibus and Wänke (1985).

Agee and Draper (2004) was depleted in Al and Ca and enriched in Fe and Mg relative to parent melts of shergottite. Therefore, neither study could show that parent melts of shergottites can be produced from DWM under their respective pressure conditions. Based on the melting study of DWM, Agee and Draper (2004) concluded that DWM is too Fe-rich to represent the Martian mantle. This conclusion is supported by Musselwhite et al. (2006). However, the experimental condition of Agee and Draper (2004) is limited at 5 GPa in pressure, which condition may be too high to represent the uppermost mantle in the Mars. Consequently, a definitive model for primitive Martian mantle composition has not been developed.

In this study, we have performed partial melting experiments on the DWM composition revisited at pressures ranging from 1.0 to 4.5 GPa under oxygen fugacities estimated from Martian meteorites (e.g., Goodrich et al., 2003; Righter et al., 2008). Our purpose was to obtain the phase relations and melt compositions as a function of degree of melting at a wide pressure range. We then directly compared the chemical trends of partial melts obtained in our high-pressure experiments with those of shergottites in an attempt to determine which, if any, basaltic shergottites actually represent a primitive (parent) melt of the Martian mantle.

EXPERIMENTAL METHOD

Starting material

The Martian mantle composition proposed by Dreibus and Wänke (DWM; 1985) was selected as the target composition of the starting material in this study. We synthesized the DWM within the SiO_2–TiO_2–Al_2O_3–Cr_2O_3–FeO–MgO–CaO–Na_2O system. Table 1 shows the DWM composition and the synthesized starting material composition. The starting material was prepared from reagent grade SiO_2, TiO_2, Al_2O_3,Cr_2O_3, Fe_2O_3, MgO, $CaCO_3$, and Na_2CO_3, which were mixed in an appropriate ratio and ground in an agate mortar and pestle under ethanol. The mixture was then dried and decarbonated in a 1-atm furnace at 800–1000 °C for 20 h in air. The dried sample was ground again in ethanol, and reduced in a 1-atm furnace at 1000 °C for 5 h and quenched with oxygen fugacity controlled at the QFM-1 buffer using CO_2/H_2 gas mixture. The reduced sample was ground in ethanol again and was kept in glass vials in a 110 °C oven. The amount of H_2O and CO_2 remaining in the synthesized starting material was measured via Fourier transform infrared spectroscopy (FTIR). No H_2O or CO_2 peaks were detected, which indicates that H_2O and CO_2 were not included in the starting materials.

In general, Pt capsule which is refractory enough to conduct high-temperature experiments have been used for melting experiments of the refractory materials such as peridotites (e.g., Jaques and Green, 1980) for a long time. But it is well known that the amount of Fe lost from silicate melts to Pt capsule is significant. Therefore, Agee and Draper (2004) used a graphite sleeve as a sample container to eliminate Fe-loss in high-temperature experiments, though the use of the graphite capsule imposed a low f_{O_2} on the sample (e.g., Matsukage and Kubo, 2003). In this study, Re/Pt double capsule was used instead of graphite as sample container to eliminate the Fe-loss (Matsukage and Kubo, 2003). The starting material was loaded into a Re container with an inner diameter of 1.4 mm constructed from Re foil 0.025 mm thick, which was then encased in a sealed Pt tube with an inner diameter of 1.6 mm and thickness of 0.2 mm. This double capsule system has been shown to provide an f_{O_2} between QFM and QFM-3 in high-pressure and -temperature melting experiments (Matsukage and Kubo, 2003) and was therefore used to maintain an oxygen fugacity close to that inferred for the Martian mantle of between QFM and QFM-4 (Goodrich et al., 2003).

Advance Publication Article

High-pressure and -temperature experiments

High-pressure and -temperature experiments at 3.0 GPa and 4.5 GPa were conducted by using a Kawai-type multi-anvil apparatus (Orange 1000) installed at Geodynamics Research Center, Ehime University. Pressure was generated by eight 26 mm tungsten carbide anvils (Toshiba F grade) with a truncated edge length of 11 mm. A Co-doped semi-sintered MgO octahedron with an 18 mm edge length was used as a pressure medium. A graphite sleeve was used as a heater and was inserted in a $LaCrO_3$ thermal insulation sleeve to reduce potential temperature gradients. The sample container was electrically insulated from the furnace by enclosing it in an MgO sleeve, and was placed in the central hot spot part of the furnace. Pressure was estimated by using load-pressure calibration, and temperature for each experiment was measured by a thermocouple. The pressure calibration was performed by using the phase transitions of Bi (2.55 GPa and 7.7 GPa) at room temperature and the quartz-coesite phase transition at 1200 °C and 3.2 GPa (Akaogi et al., 1995). Temperature was measured by a W_3Re-$W_{25}Re$ thermocouple. The error in the pressure estimate originates from uncertainties in the absolute pressure scale and the imperfect reproducibility in the experiments. It was estimated to be less than ~ 0.5 GPa. The temperature gradient in the sample capsule was estimated to be less than about ~ 50 °C.

The experiments at 1 GPa and 2.5 GPa were conducted by using a non-end-loaded piston-cylinder apparatus (ET type) and a Boyd-England-type piston-cylinder apparatus installed at the Magma Factory, Tokyo Institute of Technology (Takahashi, 1993). The pressure-load relations for the piston-cylinder apparatuses were presented by Matsukage and Kubo (2003). The experiments were performed with a 1/2 inch diameter cell assembly. The assembly included a talc and Pyrex glass outer sleeve and ALSIMG (Al and Si-doped MgO) inner sleeve with a 31 mm-long straight graphite sleeve heater with 5 mm inner diameter and 1 mm wall thickness. Temperature was measured by a W_5Re-$W_{26}Re$ thermocouple.

Chemical analysis

The run products were sectioned longitudinally and were polished for analysis. Residual minerals and quenched partial melts, which are a mixture of glass and quenched crystals, were analyzed by using a scanning electron microprobe analyzer (JEOL-JSR1000) with an energy dispersive spectrometer (Oxford) at Ehime University under a 15 kV accelerating voltage, a 0.85×10^{-8}A beam current, an integration counting time of 100 s, and a working distance of 20 mm with ZAF correction. Standards used were wollastonite for Si and Ca, rutile for Ti, corundum

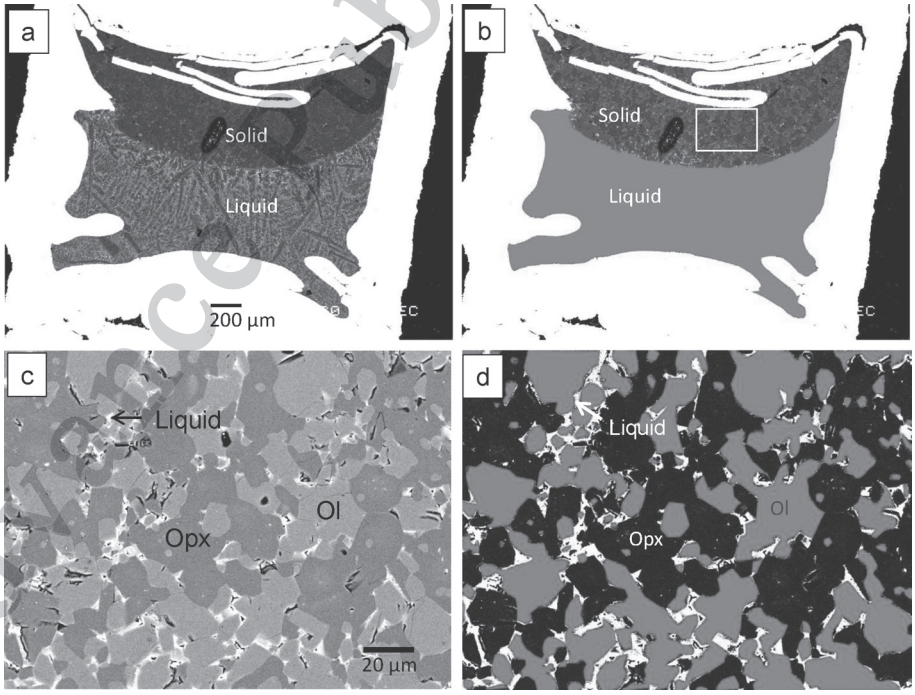

Figure 2. Images of run product (OD879) before (a), (c) and after (b), (d) image processing through Adobe Photshop CS3. (c), (d) are enlargements of the rectangular area in (b). Color version of Figure 2 is available online from http://japanlinkcenter.org/DN/JST.JSTAGE/jmps/120820.

Advance Publication Article

for Al, chromian spinel for Cr, hematite for Fe, periclase for Mg, albite for Na, and nickel oxide for Ni. A focused beam was chosen for analysis of residual minerals. The quenched partial melts became mixtures of quenched crystals and glasses. Therefore these mixtures were analyzed by scanning the beam across 20 × 20 μm to 200 × 200 μm raster areas depending on size of the melt pools that segregated from residual minerals (Fig. 2a).

Determination of degree of partial melting

Degree of partial melting was determined by two different methods; mass balance calculation and area counting. The mass balance method used compositions of the coexisting phases and bulk composition, and the degree of partial melting (M^{melt}) and modal composition of solid phases (M^j) were calculated by solving the following equation:

$$\sum_i [(X^{i,\,bulk} - (M^{melt} X^{i,\,melt} + \sum_j M^j X^{i,\,j})]^2 = \text{minimum} \quad (1)$$

where $X^{i,\,bulk}$, $X^{i,\,melt}$ and $X^{i,\,j}$ are weight % of components i in bulk rock, melt phase, and coexisting solid phases j, respectively, in the run products. SiO_2, TiO_2, Al_2O_3, Cr_2O_3, MgO, CaO, and Na_2O were used as components i in the calculation. Although the Re/Pt double capsules mostly eliminate Fe-loss, it is possible to react slightly with Fe in partial melt at higher temperature (Matsukage and Kubo, 2003). Therefore we did not use the FeO component for mass balance calculation. To compare the calculated bulk FeO with the FeO in the starting material, the degree of Fe-loss was estimated (Table 2).

The area counting method analyzed sections of run products by using Back-Scattered Electron Imaging (BEI) combined with compositional mapping of characteristic X-rays of Si, Mg, Fe, Ca, and Al. The resolution of the BEI was 1280 × 960 pixels. Figure 2 (color version is available online from http://japanlinkcenter.org/DN/JST.JSTAGE/jmps/121125) shows an example of images before and after image processing through Adobe Photoshop CS3. The partial melt was generally distributed between grain boundaries of residual crystals in run products (Figs. 2c and 2d). In those at higher temperature and thus higher degree of melting, the partial melt existed in segregated

Table 2. Run condition and results of melting experiments on DWM

Run No.	Pressure	Temperature	Duration	Run products	Degree of melting		K_D[b]	Fe loss
	(GPa)	(°C)	(hour)		AC (vol%)	MBC (wt%)		(wt%)
AK331	1.0	1300	12	Liq, Ol, Opx, Sp	9	14	0.25	< 1
AK330	1.0	1400	6	Liq, Ol, Opx, Sp	21	31	0.21	< 1
AK328	1.0	1500	2	Liq, Ol	66	60	0.27	1.2
P813	2.5	1350	12	Ol, Opx, Cpx, Sp	0	0		< 1
P812	2.5	1600	3	Liq, Ol, Opx	47	48	0.34	< 1
P815	2.5	1650	3	Liq, Ol	93	89	0.35	6.9
OD940	3.0	1396[a]	6	Liq, Ol, Opx, Cpx, Gt, Sp	< 1			< 1
OD938	3.0	1450	6	Liq, Ol, Opx	28	33	0.33	< 1
OD937	3.0	1500	6	Liq, Ol, Opx	56	57	0.35	< 1
OD864	4.5	1400	24	Ol, Opx, Cpx, Gt	0	0		< 1
OD883	4.5	1500[a]	24	Liq, Ol, Opx, Cpx, Gt	4	14	0.35	< 1
OD850	4.5	1550	6	Liq, Ol, Opx, Cpx, Gt	22	20	0.34	< 1
OD857	4.5	1600	1.8	Liq, Ol, Opx	52	59	0.33	< 1
OD879	4.5	1650[a]	2	Liq, Ol, Opx	58	56	0.34	< 1
OD900	4.5	1700	1	Liq, Ol	94	83	0.35	< 1
OD903	4.5	1750	1	Liq	100	100		2.2

Abbreviations: AC = area counting method; MBC = Mass balance calculation method.

[a] Temperature was estimated by relation between temperature and power in heating of other experiments.

[b] $K_D = X_{Mg}(liq)^* X_{Fe}(ol)/X_{Mg}(ol)^* X_{Fe}(liq)$

Advance Publication Article

melt pool in addition to grain boundaries (Figs. 2a and 2b). The interstitial melts and segregated melts were interconnected in all run products. The degree of partial melting was taken as the sum of the segregated melt and the interstitial melt. As listed in Table 2, degrees of melting obtained by the two methods were in reasonable agreement. In this study, we used the results of mass balance calculation method for discussion.

RESULTS

Melting phase relation of DWM

Table 2 lists the run conditions, phase relations and degree of melting of run products for each experiment conducted in this study. The melting phase relations of DWM are summarized in Figure 3. The subsolidus assemblage at pressure less than 2.5 GPa was olivine + orthopyroxene + clinopyroxene + spinel, while at 4.5 GPa the assemblage was olivine + orthopyroxene + clinopyroxene + garnet.

The initiation of partial melting was identified by a small amount of interstitial glass and quenched crystals at grain boundaries between residual minerals. Solidus temperature increased with increasing pressure from 1300 °C at 1.0 GPa to ~ 1500 °C at 4.5 GPa. Above the solidus, clinopyroxene melted preferentially relative to olivine and orthopyroxene. Spinel was the major Al-bearing phase at lower pressure, and its stability field extended up to 1400 °C at less than 3.0 GPa. At 3.0 GPa and 1396 °C, garnet was the dominant Al-bearing phase, although it coexisted with small amounts of fine grained chromian spinel of less than 2 μm in diameter. Therefore the phase boundary between the spinel and garnet stability fields existed at ~ 3.0 GPa. The upper temperature stability limit of garnet increased with increasing pressure. At all pressures, the phase assemblage changed from olivine + orthopyroxene + liquid to olivine + liquid with increasing degree of melting.

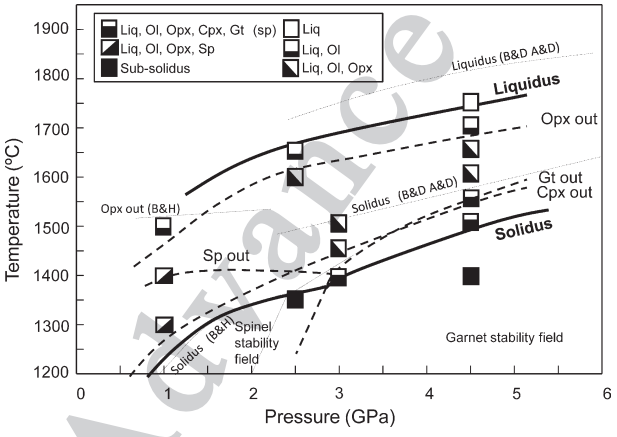

Figure 3. Melting phase relations of Martian mantle (DWM). Solidus and liquidus lines obtained inour study are compared with those of previous studies. Abbreviations: B&D, Borg and Draper (2003); A&D, Agee and Draper (2004); B&H, Bertka and Holloway (1994).

Chemistry of partial melts and residual solids

Table 3 lists the chemical compositions of all run products. In this study, we estimated the amount of Fe loss via the mass balance calculation method by using the chemical composition of coexisting phases in run products to determine the percentage of Fe lost to the capsule. As listed in Table 2, we established that the degree of Fe loss of our run products was less than 1.2 wt% except for OD903 (4.5 GPa, 1750 °C) and P815 (2.5 GPa, 1650 °C). This result indicates that the Re foil effectively eliminated the reaction between the Pt capsule and Fe in the sample in all but the highest temperature experiments.

Figure 4 plots chemical composition of partial melts of DWM at 1.0, 3.0 and 4.5 GPa, excluding OD903. Contour lines of degree of melting and chemical trends at each pressure, which were calculated by the method of Herzberg and Zhang (1996), are also shown in Figure 5. The chemical compositions of partial melts were systematically related to pressure. The low-degree melt at a lower pressure of 1.0 GPa was characterized by a high Al_2O_3 content and a low CaO/Al_2O_3 ratio (Fig. 5a). At higher pressures of 3.0 GPa and 4.5 GPa, the Al_2O_3 content in partial melt was reduced remarkably with increasing pressure, although the CaO content did not change significantly (Fig. 5b). Therefore, the CaO/Al_2O_3 ratio increased with increasing pressure. The influence of the Al-rich solidus phase can be considered as the most important cause of the pressure dependence of Al_2O_3 content in low-degree melts. In the spinel stability field, Al in spinel was dominantly distributed into the partial melt. Therefore the formation of Al_2O_3-rich melt was accompanied by the formation of Cr-rich residual spinel (Table 3 and Fig. 4). The residual chromian spinel was more refractory relative to the Al-rich spinel so that its stability field spreaded to higher temperature (Fig. 3). Above 3 GPa, on the contrary, garnet was stable as a solidus phase instead of spinel. In this case, Al remained in the residual garnet (Table 3 and Fig. 4), which coexisted with Al-poor partial melt. Garnet would become more refractory with increasing pressure. The low-degree melts had low Mg# [= Mg/(Mg + Fe) atomic ratio], which increased with increasing degree of melting (Figs. 5c and 5d). Both FeO and MgO contents in the partial melts increased with increasing pressure (Fig. 5d). It is noteworthy that partial melts at higher pressures were characterized by a relatively high

Advance Publication Article

FeO content (Fig. 5c). The melt compositions approached that of the starting material with an increasing degree of melting.

As listed in Table 3, the Mg# of residual olivine, pyroxenes and garnet gradually increased with increasing degree of melting (increasing temperature). The CaO content of clinopyroxene was lower than that observed in the terrestrial mantle and tended to decrease with increasing temperature. As described above, the Cr# [= Cr/(Cr + Al) atomic ratio] of spinel increased with increasing degree of melting, from 0.37 at subsolidus condition to 0.82 at more than 30% of degree of melting. The garnet was rich in components of pyrope ($Mg_3Al_2Si_3O_{12}$) and almandine ($Fe^{2+}_3Al_2Si_3O_{12}$), with small amounts of uvarovite ($Ca_3Cr_2Si_3O_{12}$) and andradite ($Ca_3Fe^{3+}_2Si_3O_{12}$) components. The Cr# of garnet did not change with increasing degree of melting (Table 3).

DISCUSSION AND CONCLUSION

Comparison with previous melting studies of the Martian mantle

Figure 3 compares the melting phase relations from this investigation with those of previous studies (Bertka and Holloway, 1994a; Borg and Draper, 2003; Agee and Draper, 2004). Bertka and Holloway (1994a) determined the solidus temperature of DWM at pressure less than 3 GPa, while Borg and Draper (2003) and Agee and Draper (2004) reported the solidus and liquidus temperatures of L chondrite Homestead L5 at pressure more than 5 GPa and 3 GPa, respectively. In experimental studies by Borg and Draper (2003) and Agee and Draper (2004), Homestead L5 was used as analog of the Martian mantle because the chemistry of Homestead L5 is similar to that of DWM. Our results are in good agreement with those of Bertka and Holloway (1994a) but contradict those of Borg and Draper (2003) (Fig. 3). The difference in solidus temperature observed in this research and that in the previous study on Homestead L5 is approximately 80 °C at 4.5–5 GPa. At present, the reason for this discrepancy remains unclear; however, it is likely the result of compositional differences in starting materials. The difference of melt detection method could be an addition factor in this discrepancy.

Figure 5 compares the chemical compositions of partial melts observed in this work with those of previous studies (Bertka and Holloway, 1994b; Agee and Draper, 2003). As described in the results section, the chemical compositions of partial melts changed markedly with pressure, whereby Al_2O_3 decreased and FeO increased as pressure increased (Figs. 5a and 5c). This pressure dependence is consistent with the results of previous studies.

Comparison with Martian basaltic rocks

To evaluate whether basaltic shergottites are representative of a partial melt of DWM, the bulk chemistries of the shergottites (Fig. 1) were compared with the chemical trends of partial melts of DWM obtained from our experiments at 1.0–4.5 GPa (Fig. 6). As previously described, basaltic shergottites are divided into olivine-bearing and olivine-free basalts. The olivine-bearing shergottites generally have a porphyritic texture characterized by the presence of larger olivine crystals in a fine-grained matrix of pyroxenes and plagioclase crystals ± glass (olivine-phyric shergottites of Goodrich, 2002). Not all olivine-bearing shergottites, however, exhibit such a texture. For example, the grain size of olivine in NWA5990 is only slightly larger than the coexisting pyroxene (Irving et al., 2010b). Olivine-phyric and olivine-free shergottites are also clearly divided in their bulk chemistries. In general, the contents of Al_2O_3 and CaO are higher, and MgO is lower in olivine-free shergottites than those in olivine-phyric shergottites. However, the FeO content is comparable between the two types of basaltic shergottites (Fig. 1).

Because of the high Mg# in the bulk rock composition (Fig. 1b), several researchers consider that some of the olivine-phyric shergottites are primitive melts originating from the Martian mantle (e.g., Zipfel et al., 2000; Irving et al., 2002, 2010b; Misawa, 2004). Figure 6 compares the partial melt trends of DWM with the bulk composition of Yamato980459, which is composed of coarse olivine and pyroxene crystals with high-Mg# in a fine-grained glassy groundmass. Yamato980459 is characterized by a low Al_2O_3 content and high CaO/Al_2O_3 ratio. Therefore, on the basis of the relationship between CaO and Al_2O_3 contents, Yamato980459 would be estimated as ~ 30–40% partial melt of DWM at pressures of 3–4.5 GPa (Figs. 6a and 6b). However, this result is not consistent with the estimation resulting from the Mg# and FeO relationship (Fig. 6c), which suggests that it would have formed as a ~ 60–70% melt of DWM at ~ 1 GPa. Thus, our results indicate that it is difficult to form a melt with the composition of Yamato980459 via partial melting and subsequent melt extraction processes if actual Martian mantle composition is similar to that of DWM. It also suggests that some of the other olivine-phyric shergottites with bulk chemistry of major elements resembling that of Yamato980459 are also unlikely to be primitive melts of DWM. If olivine-phyric shergottite with low Al_2O_3 and high CaO/Al_2O_3 is truly a direct mantle melt composition, a mantle composition other than that of DWM must be

Advance Publication Article

Table 3. Chemical and modal compositions of experimental liquid and residual mineral phases

Run No.	(wt%)	Mode	SiO_2	TiO_2	Al_2O_3	Cr_2O_3	FeO	MgO
AK331	Liq	14	45.2 (0.9)	0.9 (0.1)	12.0 (1.2)	0.0 (0.0)	15.8 (1.2)	7.2 (2.9)
	Ol	48	38.4 (0.6)		0.0 (0.0)	0.0 (0.1)	22.0 (0.4)	40.0 (0.5)
	Opx	37	53.6 (1.3)		2.5 (0.5)	1.1 (0.2)	12.9 (0.4)	28.3 (0.6)
	Sp	1	3.20 (1.0)	0.6 (0.1)	19.3 (2.1)	40.3 (1.8)	25.5 (0.3)	10.3 (0.2)
AK330	Liq	31	47.2 (2.3)	0.3 (0.3)	8.9 (0.8)	0.3 (0.3)	20.3 (0.4)	9.9 (1.8)
	Ol	51	39.3 (0.7)		0.0 (0.0)	0.1 (0.2)	18.3 (0.4)	43.3 (0.7)
	Opx	32	55.9 (0.6)		0.9 (0.2)	0.8 (0.2)	10.3 (0.5)	32.0 (0.7)
	Sp	<1	0.5 (0.1)	0.0 (0.0)	8.3 (0.1)	57.0 (0.7)	23.9 (0.2)	10.1 (0.1)
AK328	Liq	59	48.6 (3.2)	0.1 (0.2)	5.2 (0.8)	1.1 (0.2)	18.8 (1.6)	19.2 (4.2)
	Ol	41	39.4 (1.1)		n.d.	0.5 (0.4)	12.5 (0.5)	46.7 (1.2)
P813	Ol	45	38.4 (0.8)		0.3 (0.0)	0.4 (0.6)	22.3 (0.6)	39.5 (1.0)
	Opx	31	52.0 (1.6)		5.1 (0.5)	0.9 (0.2)	13.8 (0.7)	26.5 (0.4)
	Cpx	23	51.6 (1.6)	0.1 (0.2)	4.7 (0.2)	1.0 (0.2)	12.4 (0.6)	21.3 (1.8)
	Sp	1	0.7 (0.3)	1.3 (0.0)	27.6 (1.5)	23.8 (0.8)	33.3 (0.4)	11.3 (0.2)
P812	Liq	48	44.2 (0.8)	0.0 (0.0)	5.4 (0.3)	1.0 (0.1)	19.7 (1.5)	18.3 (1.1)
	Ol	39	39.0 (1.2)		0.1 (0.2)	0.4 (0.4)	15.9 (0.3)	43.9 (0.7)
	Opx	13	53.9 (0.7)		2.3 (0.8)	1.1 (0.3)	10.0 (0.4)	30.5 (0.9)
OD940	Ol		39.0 (0.9)		0.1 (0.2)	0.2 (0.4)	21.3 (0.7)	40.2 (1.1)
	Opx		54.0 (1.0)		3.3 (0.2)	1.3 (0.2)	12.8 (0.6)	27.5 (0.4)
	Cpx		54.0 (1.2)	0.0 (0.0)	3.9 (0.4)	1.3 (0.2)	11.5 (0.5)	21.7 (1.3)
	Gt		40.9 (0.8)	0.2 (0.3)	19.7 (0.6)	3.4 (0.7)	13.7 (1.0)	16.6 (0.4)
OD938	Liq	33	42.7 (1.3)	0.4 (0.2)	6.4 (0.2)	0.8 (0.2)	22.6 (0.9)	16.8 (0.5)
	Ol	40	39.0 (0.3)		0.0 (0.0)	0.3 (0.3)	18.3 (0.4)	42.0 (0.4)
	Opx	27	53.8 (0.9)		2.7 (0.4)	1.3 (0.2)	11.4 (0.4)	28.6 (0.7)
OD937	Liq	57	44.0 (1.3)	0.1 (0.2)	5.0 (0.2)	0.9 (0.1)	19.9 (0.4)	21.1 (0.4)
	Ol	33	39.8 (0.5)		0.0 (0.0)	0.3 (0.3)	14.8 (0.4)	45.4 (0.6)
	Opx	11	55.8 (1.0)		1.7 (0.3)	1.1 (0.2)	9.8 (0.5)	31.5 (0.6)
OD864	Ol	46	38.3 (1.0)		0.0 (0.0)	0.0 (0.0)	23.3 (1.0)	39.5 (0.9)
	Opx	31	54.6 (0.5)		1.5 (0.1)	0.6 (0.1)	14.0 (0.4)	28.0 (0.3)
	Cpx	10	53.9 (0.8)	0.1 (0.1)	2.2 (0.1)	1.0 (0.2)	11.1 (0.5)	18.5 (0.4)
	Gt	13	39.9 (0.4)	0.5 (0.1)	18.0 (0.4)	4.5 (0.4)	16.6 (0.5)	16.2 (0.4)
OD883	Liq	14	41.8 (4.5)	0.8 (0.2)	4.4 (0.5)	0.5 (0.1)	21.8 (4.5)	15.7 (0.8)
	Ol	42	39.2 (1.1)		0.0 (0.0)	0.0 (0.0)	20.1 (0.8)	41.5 (1.2)
	Opx	28	54.3 (0.5)		2.4 (0.1)	0.9 (0.1)	12.4 (0.5)	28.5 (0.1)
	Cpx	7	53.7 (1.1)	0.0 (0.1)	2.9 (0.0)	1.0 (0.0)	12.1 (0.1)	22.6 (1.0)
	Gt	9	41.8 (0.6)	0.0 (0.1)	19.1 (1.0)	4.2 (0.2)	13.6 (0.1)	18.3 (0.1)
OD850	Liq	20	39.7 (0.9)	0.5 (0.3)	4.1 (0.3)	0.6 (0.1)	24.8 (1.3)	18.2 (1.0)
	Ol	39	39.6 (1.0)		0.0 (0.0)	0.2 (0.3)	19.4 (0.5)	41.7 (1.7)
	Opx	30	53.0 (2.5)		2.2 (0.1)	0.9 (0.0)	11.7 (0.5)	27.5 (1.3)
	Cpx	3	54.2 (0.3)	0.0 (0.1)	2.4 (0.0)	1.1 (0.1)	11.7 (0.0)	23.9 (0.1)
	Gt	8	40.8 (0.6)	0.0 (0.1)	18.3 (0.4)	4.5 (0.0)	13.2 (0.2)	18.1 (0.1)
OD857	Liq	59	42.9 (0.6)	0.1 (0.2)	4.6 (0.1)	1.0 (0.0)	20.3 (0.2)	22.2 (0.2)
	Ol	27	40.0 (2.6)		0.0 (0.0)	0.4 (0.1)	14.0 (0.1)	45.9 (3.6)
	Opx	13	54.8 (3.1)		1.5 (0.2)	0.8 (0.1)	8.5 (0.4)	31.9 (2.2)
OD879	Liq	56	44.3 (1.5)	0.2 (0.2)	4.6 (0.1)	1.0 (0.1)	21.0 (1.0)	22.4 (0.3)
	Ol	29	40.1 (2.0)		0.0 (0.0)	0.3 (0.3)	14.6 (1.0)	45.6 (1.4)
	Opx	15	55.8 (2.8)		2.0 (0.2)	0.9 (0.1)	9.1 (0.4)	32.2 (1.4)
OD900	Liq	83	46.4 (0.4)	0.1 (0.2)	3.3 (0.1)	0.9 (0.1)	18.3 (0.2)	26.9 (0.3)
	Ol	17	40.3 (3.7)		0.0 (0.0)	0.2 (0.3)	11.4 (0.5)	48.2 (4.4)

Abbreviations: Liq, liquid; Ol, olivine; Opx, Mg-rich pyroxene; Cpx, Ca pyroxene; Sp, chromian spinel; Gt, garnet; Mg#, Mg/(Mg + Fe) atomic ratio.

Advance Publication Article

CaO		Na_2O		Total	Mg#
12.3	(0.9)	2.2	(1.0)	95.6	0.450
0.3	(0.2)			100.7	0.764
1.8	(0.2)			100.3	0.796
0.6	(0.4)	0.5	(0.1)	100.3	
8.5	(0.8)	1.6	(0.2)	97.0	0.465
0.1	(0.1)			101.0	0.808
0.7	(0.1)			100.6	0.848
0.1	(0.2)			99.9	
4.1	(1.0)	1.9	(0.4)	99.1	0.646
n.d.				99.1	0.869
0.3	(0.3)			101.2	0.760
2.0	(0.2)			100.4	0.773
7.7	(1.7)	1.6	(0.1)	100.4	0.755
0.0	(0.0)			98.1	
4.8	(0.3)	1.0	(0.1)	94.4	0.624
0.1	(0.1)			99.4	0.831
1.2	(0.3)			98.9	0.845
0.2	(0.1)			101.0	0.771
2.0	(0.1)			100.8	0.793
8.6	(1.6)	0.7	(0.2)	101.7	0.770
5.3	(0.3)	n.d.		99.9	0.683
6.9	(0.5)	0.9	(0.3)	97.5	0.570
0.1	(0.1)			99.7	0.803
1.5	(0.1)			99.2	0.818
4.8	(0.1)	0.5	(0.0)	96.3	0.653
0.0	(0.0)			100.3	0.845
0.9	(0.1)			100.8	0.851
0.0	(0.1)			101.1	0.751
1.7	(0.1)			100.3	0.781
11.7	(0.5)	2.0	(0.0)	100.5	0.748
5.2	(0.3)	0.5	(0.4)	101.4	0.636
9.2	(1.7)	1.4	(0.4)	95.6	0.562
0.2	(0.3)			101.0	0.786
1.7	(0.0)			100.2	0.804
6.8	(0.6)	1.4	(0.1)	100.5	0.768
4.6	(0.0)	0.5	(0.1)	102.1	0.706
7.1	(0.3)	1.2	(0.1)	96.2	0.567
0.0	(0.0)			101.0	0.793
1.7	(0.0)			97.0	0.808
5.7	(0.3)	1.2	(0.1)	100.1	0.785
4.4	(0.1)	0.5	(0.1)	99.7	0.71
4.3	(0.1)	0.7	(0.1)	96.1	0.660
0.0	(0.0)			100.3	0.853
0.8	(0.1)			98.3	0.869
4.5	(0.1)	1.2	(0.6)	99.2	0.656
0.0	(0.0)			100.6	0.847
1.0	(0.1)			100.9	0.864
2.9	(0.2)	0.7	(0.1)	99.6	0.723
0.0	(0.0)			100.1	0.883

the source (e.g., Musselwhite et al., 2006).

The results of this study suggest that two shergottites, NWA5990, QUE94201, could have the primitive melt compositions of DWM (Fig. 6). NWA5990 is an olivine-bearing diabasic igneous rock composed mainly of clinopyroxene, plagioclase and olivine with accessory opaque minerals such as chromian spinel (Irving et al., 2010b). NWA5990 differs from other olivine-bearing shergottites in major element chemistry (Figs. 1 and 6). The Mg# and CaO/Al_2O_3 are lower while Al_2O_3 and FeO contents are higher in NWA5990 than in those of Yamato980459. By using the relationship of degree of melting and chemical trends of partial melts obtained in our experiments (Fig. 6), NWA5990 could have originated as a possible melt formed by 30–40% partial melting of DWM at ~ 2 GPa. However, this theory is not plausible because such a large degree of melting requires special circumstances to prevent the melt from separating from the surrounding crystals (e.g., Longhi, 1995). QUE94201 is an olivine-free basaltic shergottite dominated by pyroxenes and plagioclase (Kring et al., 2003). On the basis of petrographic and chemical observations, QUE94201 is considered to represent a bulk melt rather than a cumulate fraction. In this sample, the Mg# and CaO/Al_2O_3 are lower than those in olivine-bearing shergottites, while its Al_2O_3 content is higher (Figs. 1 and 6). These compositional features of QUE94201 can be reproduced in a low-degree (<20%) partial melt of DWM formed at low pressure (~ 1 GPa; Fig. 6). The melting condition is estimated at approximately 1355 °C at 1.0 GPa for QUE94201-like melt, if the actual Martian mantle is similar in composition to that of DWM.

Basaltic rocks have been described from the Spirit landing site at Gusev Crater (McSweenet at., 2004), and their petrological features have been reported precisely by McSween et al. (2006). The Gusev basalts are estimated to be mainly composed of olivine, pyroxenes and plagioclase, which is comparable to the mineralogy of olivine-phyric shergottites. The chemistries of the Gusev basalts, however, differ strongly from those of olivine-phyric shergottites, with the former having a higher Al_2O_3 content and lower Mg# (Fig. 6). As shown in Fig. 6, these basalts may be consistent with a ~ 20–30% partial melt of DWM in the spinel stability field at ~ 1.0 GPa, although the CaO/Al_2O_3 ratio is slightly lower than the melt trend at that pressure. To understand the formation conditions of the Gusev basalts, Monders et al. (2007) and Filiberto et al. (2008) performed crystallization experiments on synthetic Gusev basalts at high pressure. Monders et al. (2007) reported that one of the Gusev basalts, Adirondack, is multiply saturated with olivine (Mg# = 0.74), orthopyroxene (Mg# = 0.77) and spinel (Cr# = 0.59) near

Advance Publication Article

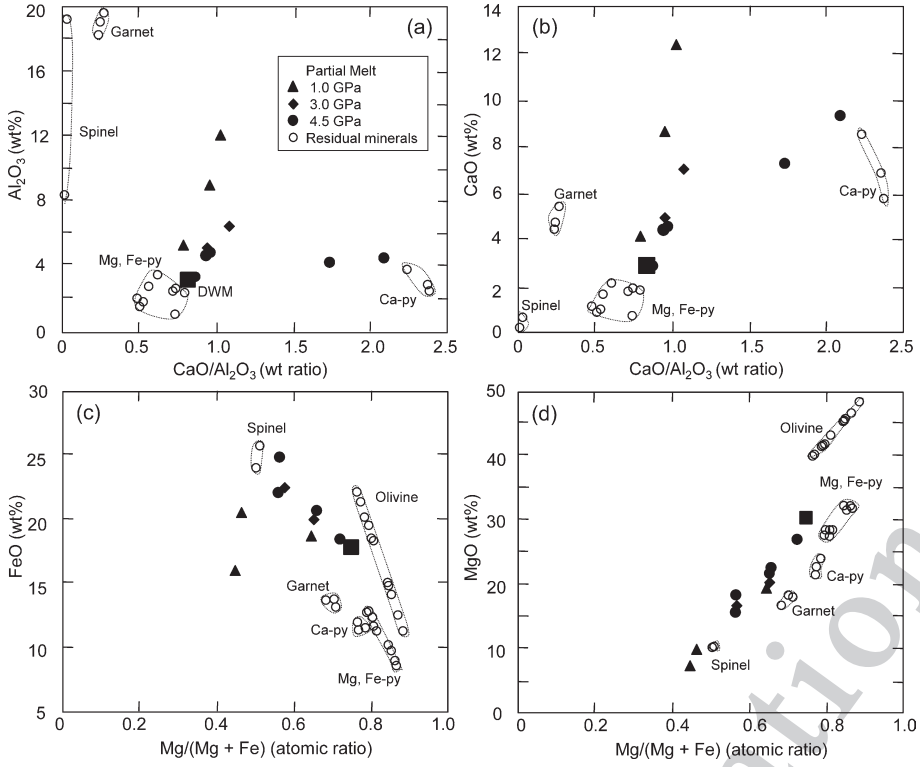

Figure 4. Chemical compositions of partial melts and residual minerals produced by partial melting of Martian mantle (DWM) at 1, 3 GPa and 4.5 GPa. Abbreviations: Mg, Fe-py, Mg and Fe-rich pyroxene; Ca-py, Ca-rich pyroxene.

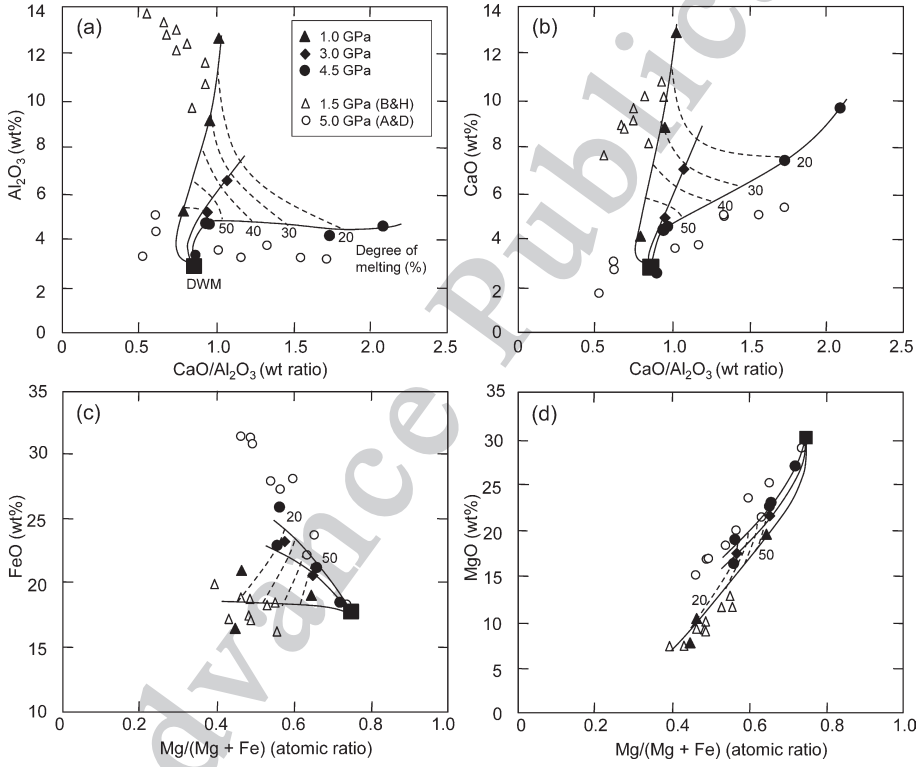

Figure 5. Chemical compositions of liquids produced by partial melting of Martian mantle (DWM) at 1, 3 and 4.5 GPa, compared with previous studies at 1.5 GPa by Bertka and Holloway (1994) and at 5 GPa by Agee and Draper (2004). Broken lines and solid lines indicate contour lines of degree of melting and chemical trends of each pressure, respectively.

its liquidus at 1320 °C and 1.0 GPa. In our experiments at 1300 °C and 1.0 GPa, the residual mineral assembly of DWM is olivine (Mg# = 0.76) + orthopyroxene (Mg# = 0.79) + spinel (Cr# = 0.58; see Table 3). Although the constituent minerals and Cr_2O_3 content in spinel agree well with each other, the MgO content in olivine and orthopyroxene of Adirondack basalt are lower than those of residual minerals of DWM. It is widely accepted that the

Advance Publication Article

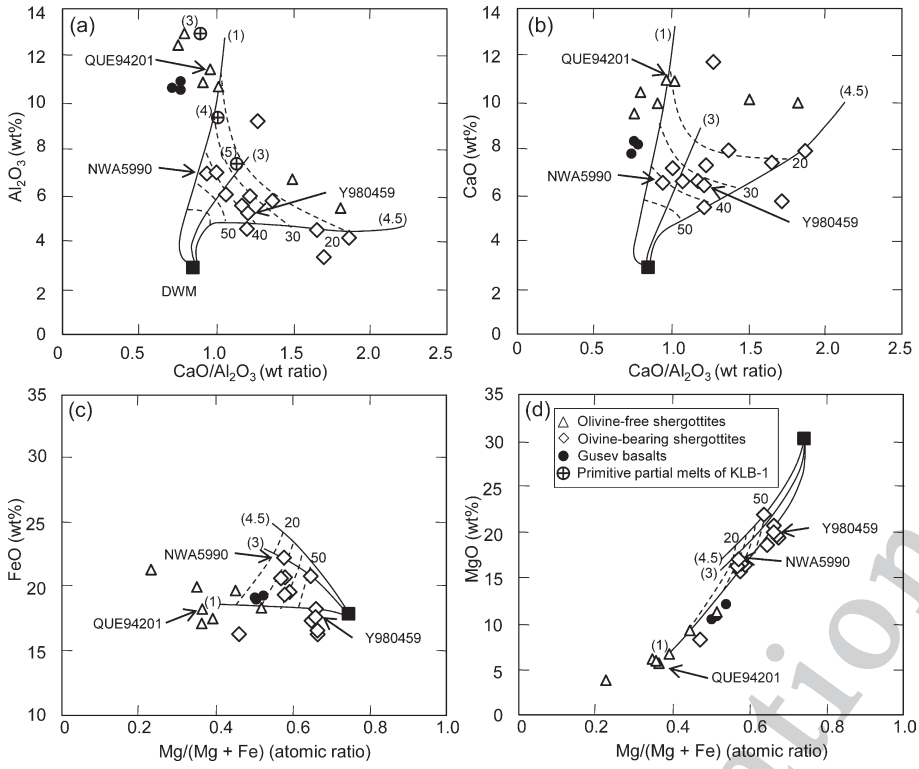

Figure 6. Comparison of chemical compositions of partial melt trends of DWM with Gusev basalts, olivine-free and olivine-phyric basaltic shergottites. Data for Gusev basalts and primitive partial melts of KLB-1 at 3-5 GPa are after McSween et al. (2006) and Herzberg and Zhang (1996), respectively. References for shergottites are the same as those listed in Figure 1. Numbers with and without parenthesis indicate pressure and degree of melting, respectively.

Cr# of spinel coexisting with olivine ± pyroxene in basaltic magma is nearlyconstant with a rapid decrease in the Mg# of olivine ± pyroxene by even a small degree of crystal fractionation at the early stage of the fractionation process (e.g., Arai, 1994). Therefore, if the actual Martian mantle is similar in composition to that of DWM, the Adirondack basalts can be explained as a melt that experienced a small amount of crystal fractionation in the shallower Martian mantle (Filiberto et al., 2008).

As mentioned in the Introduction, resent estimations have suggested that the Martian mantle may actually have a higher Mg# (0.77–0.80) than that of DWM (0.75) (e.g., Yoder et al., 2003; Agee and Draper, 2004; Musselwhite et al., 2006; Minitti et al., 2007); however, its actual values remain uncertain. We consider the influence of Mg# on the primary partial melt composition. In our experiments of Fe-rich DWM at less than 5GPa, modal composition of garnet was comparable to that of clinopyroxene at temperature above the solidus (Fig. 3). However, in the partial melting of Fe-poor peridotite such as primitive lherzolite of the Earth, the modal garnet was lower than that of clinopyroxene above solidus (Walter, 1998). These observations suggest that the CaO/Al_2O_3 ratio in the partial melts at garnet stability filed decreases and Al_2O_3 increases when the Mg# of the mantle increases (Fig. 5a; Herzberg and Zhang, 1996) because the modal ratio of solidus garnet (= Al-rich phase) and clinopyroxene (= Ca-rich phase) control the CaO/Al_2O_3 ratio of coexisting partial melt (Figs. 4a and 6a). Consequently it is difficult to consider the olivine-phyric shergottites with a high-CaO/Al_2O_3 ratio and low-Al_2O_3 content (Fig. 1) as a primitive partial melt at the uppermost mantle if the actual Martian mantle has a higher Mg#.

Possible igneous process in the Martian uppermost mantle

If the conclusion is correct that the olivine-poor or -free basaltic magma with low CaO/Al_2O_3 ratio and high Al_2O_3 content are possible primitive melts, there is no reasonable crystal fractionation process that can produce the olivine-phyric shergottites with low Al_2O_3 and FeO concentrations, such as Yamato980459. If a partial melt separates and migrates upward from the residual upper mantle and cools at a shallower level in the mantle or crust, olivine is initially saturated followed by clinopyroxene crystallization. If the crystallized minerals fractionate out of the melt, the Al_2O_3 concentration in the fractionated melt would increase because the Al_2O_3 component is incompatible in olivine and not an essential structural constituent of clinopyroxene crystals.

Here, we consider that the olivine-poor or -free basaltic magmas react with the wall rocks during migration to the surface. In the Earth, reaction textures between primitive basaltic (gabbroic) magma and its surrounding wall rock peridotites are frequently observed in various

Advance Publication Article

tectonic settings (e.g., Quick, 1981; Kelemen et al., 1992; Arai and Abe, 1995; Arai and Matsukage, 1996). If a high-pressure melt ascends and then comes in contact with peridotite at a lower pressure, pyroxenes in the wall rock should be dissolved into melt from the latent heat released by the crystallization of olivine (e.g., Quick, 1981; Kelemen, 1990). High-pressure melts are generally undersaturated with pyroxene and oversaturated with olivine at low pressure (Kushiro, 1969); thus, this crystallized olivine may be entrained by the melt in the form of xenocrysts as it ascends. Through this process, a primary melt in the mantle of Mars can be modified during its migration to the surface of the planet. In this case, the olivine crystals in olivine-phyric shergottites can be considered as a mixture of xenocrysts from the melt/wall rock reaction and phenocrysts crystallized from the melt. Filiberto et al. (2010) discussed a similar process for olivine accumulation in olivine-phyric shergottite, NWA1068. Mafic to ultramafic rocks with low Al_2O_3 and high CaO/Al_2O_3 are required as wall rocks for the formation of Al_2O_3-poor olivine-phyric shergottite to occur in the Martian mantle through the melt/wall rock reaction process. Considering the results reported by Agee and Draper (2004) and those presented here, we suggest that the cumulate crystalline residue from a melt originating at higher pressure of more than 4.5GPa is one candidate for wall rock materials because the chemistry of partial melts at higher pressures are characterized by a low Al_2O_3 content and high CaO/Al_2O_3 ratio.

ACKNOWLEDGMENTS

We thank Y. Nishihara and T. Inoue for discussion and Y. Tsumagari, N. Tsujino, and M. Iehisa for help with our experiments. In addition, we thank J. Filiberto and D. Draper for their comments about the chemistry of Martian mantle. The comments made by anonymous reviewers are also appreciated. This study is partially supported by a grant-in-aid for scientific research on innovative areas (21109004).

SUPPLEMENTARY MATERIAL

Color version of Figure 2 is available online from http://japanlinkcenter.org/DN/JST.JSTAGE/jmps/120820.

REFERENCES

Agee, C.B. and Draper, D.S. (2004) Experimental constraints on the origin of Martian meteorites and the composition of the Martian mantle. Earth and Planetary Science Letters, 224, 415-429.

Akaogi, M., Yusa, H., Shiraishi, K. and Suzuki, T. (1995) Thermodynamic properties of α-quartz, coesite, and stishovite and equilibrium phase relations at high pressures and high temperatures. Journal of Geophysical Research, 100, 22337-22347.

Anand, M., James, S., Greenwood, R.C., Johnson, D., Franchi, I.A. and Grady, M.M. (2008) Mineralogy and geochemistry of shergottite RBT 04262. Lunar and Planetary Science, 39, #2173(abs).

Arai, S. (1994) Compositional variation of olivine-chromian spinel in Mg-rich magmas as aguide to their residual spinel peridotites. Journal of Volcanology and Geothermal Research, 59, 279-293.

Arai, S. and Abe, N. (1995) Reaction of orthopyroxene in peridotite xenoliths with alkali-basalt melt and its implication for genesis of alpine-type chromitite. The American Mineralogist, 80, 1041-1047.

Arai, S. and Matsukage, K. (1996) Petrology of the gabbro-troctolite-peridotite complex from hess deep, equatorial pacific: implications for mantle-melt interaction within the oceanic lithosphere. Proceedings of the Ocean Drilling Program Scientific Results, 147, 135-155.

Barrat, J.A., Blichert-Toft, J., Nesbitt, R.W. and Keller, F. (2001) Bulk chemistry of Saharan shergottite Dar al Gani 476. Meteoritics & Planetary Science, 36, 23-29.

Barrat, J.A., Jambon, A., Bohn, M., Gillet, P., Sautter, V., Göpel, C., Lesourd, M. and Keller, F. (2002) Petrology and chemistry of the Picritic Shergottite North West Africa 1068 (NWA 1068). Geochimica et Cosmochimica Acta, 66, 3505-3518.

Bertka, C.M. and Fei, Y. (1997) Mineralogy and the Martian interior up to core-mantle boundary pressures. Journal of Geophysical Research, 102, 5251-5264.

Bertka, C.M. and Holloway, J.R. (1994a) Anhydrous partial melting of an iron-rich mantle I: subsolidus phase assemblages and partial melting phase relations at 10 to 30 kbar. Contributions to Mineralogy and Petrolgy, 115, 313-322.

Bertka, C.M. and Holloway, J.R. (1994b) Anhydrous partial melting of an iron-rich mantle II: primary melt compositions at 15 kbar. Contributions to Mineralogy and Petrolgy, 115, 323-338.

Borg, L.E. and Draper, D.S. (2003) A petrogenetic model for the origin and compositional variation of the Martian basaltic meteorites. Meteoritics & Planetary Science, 38, 1713-1731.

Borisov, A. and Jones, J.H. (1999) An evaluation of Re, as an altemative to Pt, for the 1 bar loop technique; an experimental study at 1400°C. The American Mineralogist, 84, 1528-1534.

Dreibus, G., Palme, H., Rammensee, W., Spettel, B., Weckwerth, G., Wänke, H., Chemie, M. and Germany, F.R. (1982) Composition of shergotty parent body: further evidence of a two component model of planet formation. Lunar and Planetary Science, 13, 186-187 (abs).

Dreibus, G. and Wänke, H. (1985) Mars, a volatile-rich planet. Meteoritics, 20, 367-381.

Dreibus, G., Spettel, B., Wlotzka, F., Schultz, L., Weber, H.W., Jochum, K.P. and Wänke, H. (1996) QUE94201: An unusual Martian basalt. Meteoritics & Planetary Science, 31, 39-40.

Dreibus, G., Spettel, B., Haubold, R., Jochum, K.P., Palme, H., Wolf, D. and Zipfel, J. (2000) Chemistry of a new shergottite: Sayh al Uhaymir 005 (abs). Meteoritics & Planetary Science, 35, A49.

Dreibus, G., Wlotzka, F., Huisl, W., Jagoutz, E., Kubny, A. and Spettel, B. (2002) Chemistry and petrology of the most feld-

Advance Publication Article

spathic shergottite: Dhofar 378. Abstracts of the 65th annual meeting, Meteoritics & Planetary Science, 37, A43.

Easton, A.J. and Elliot, C.J. (1977) Analyses of some meteorites from the British Museum (Natural History) collection. Meteoritics, 12, 409-416.

Filiberto, J., Treiman, A.H. and Le, L. (2008) Crystallization experiments on a Gusev Adirondack basalt composition. Meteoritics & Planetary Science, 43, 1137-1146.

Filiberto, J., Musselwhite, D.S., Gross, J., Burgess, K., Le, L. and Treiman, A.H. (2010) Experimental petrology, crystallization history, and parental magma characteristics of olivine-phyric shergottite NWA1068: implications for the petrogenesis of "enriched" olivine-phyric shergottites. Meteoritics & Planetary Science, 45, 1258-1270.

Filiberto, J. and Dasgupta, R. (2011) Fe^{2+}-Mg partitioning between olivine and basaltic melts: Applications to genesis of olivine-phyric shergottites and conditions of melting in the Martian interior. Earth and Planetary Science Letters, 304, 527-537.

Folco, L., Franchi, I.A., D'orazio, M., Rocchi, S. and Schultz, L. (2000) A new martian meteolite from the Sahara: The shergottite Dar al Gani,489. Meteoritics & Planetary Science, 35, 827-839.

Goodrich, C.A. (2002) Olivine-phyric martian basalts: A new type of shergottite. Meteoritics & Planetary Science, 37, B31-34.

Goodrich, C.A. (2003) Petrogenesis of olivine-phyric shergottites Sayh al Uhaymir 005 and Elephant Moraine A79001 lithology A. Geochimica et Cosmochimica Acta, 67, 3735-3771.

Goodrich, C.A., Herd, C.D.K. and Taylor, L.A. (2003) Spinels and oxygen fugacity in olivine-phyric and lherzolitic shergottites. Meteoritics & Planetary Science, 38, 1773-1792.

Greeley, R., Foing, B.H., McSween, H.Y., Neukum, G., Pinet, P., van Kan, M., Werner, S.C., Williams, D.A. and Zegers, T.E. (2005) Fluid lava flows in Gusev crater, Mars. Journal of Geophysical Research, 110, doi:10.1029/2005JE002401.

Greshake, A., Fritz, J. and Stöffler, D. (2004) Petrology and shock metamorphism of the olivine-phyric shergottite Yamato980459: Evidence for a two-stage cooling and a single-stage ejection history. Geochimica et Cosmochimica Acta, 68, 2359-2377.

Grimm, R.E. and McSween, H. (1982) Numerical simulation of crystal fractionation in shergottite meteorites. Journal of Geophysical Research, 87, A385-392.

Gross, J., Treiman, A.H., Filiberto, J. and Herd, C.D.K. (2011) Primitive olivine-phyric shergottite NWA5789: Petrography, mineral chemistry, and cooling history imply a magma similar to Yamato-980459. Meteoritics & Planetary Science, 46, 116-133.

Hale, V.P.S., McSween, H.Y. and McKay, G.A. (1999) Re-evaluation of intercumulus liquid composition and oxidation state for the Shergotty meteorite. Geochimica et Cosmochimica Acta, 63, 1459-1470.

Haramura, H. (1995) Chemical compositions of Antarctic meteolites. In catalog of the Antarctic Meteorites (Yanai, K. and Kojima, H. Eds.). pp 48, National Institute of Polar Research, Tokyo.

Herzberg, C. and Zhang, J. (1996) Melting experiments on anhydrous peridotite KLB-1: Compositions of magmas in the upper mantle and transition zone. Journal of Geophysical Research, 101, 8271-8295.

Ikeda, Y., Kimura, M., Takeda, H., Shimoda, G., Kita, N.T., Morishita, Y., Suzuki, A., Jagoutz, E. and Dreibus, G. (2006) Petrology of a new basaltic shergottite: Dhofar 378. Antarctic Meteorite Research, 19, 20-44.

Irving, A.J., Kuehner, S.M., Hupe, A.C. and Hupe, G.M. (2002) Olivine-phyric basaltic shergottite NWA1195: A very primitive martian lava. Meteoritics & Planetary Science, 37, A69.

Irving, A.J., Kuehner, S.M., Herd, C.D.K., Gellissen, M., Korotev, R.L., Puchtel, I., Walker, R.J., Lapen, T.J. and Rumble, D. (2010a) Petrologic, elemental and multi-isotopic characterization of permafic olivine-phyric shergottite Northwest Africa 5789: A primitive magma derived from depleted Martian mantle. 41th Lunar and Planetary Science Conference, 1547.

Irving, A.J., Kuehner, S.M., Herd, C.D., Gellissen, K., Rumble, D., Lapen, T.J., Ralew, S. and Altmann, M. (2010b) Olivine-bearing diabasic shergottite Northwest Africa 5990: Petrology and composition of a new type of depleted Martian igneous rock. 41th Lunar and Planetary Science Conference, 1833.

Jaques, A.L. and Green, D.H. (1980) Anhydrous melting of peridotite at 0-15 kb pressure and the genesis of tholeiitic basalts. Contribution to Mineralogy and Petrology, 73, 287-310.

Kelemen, P.B. (1990) Reaction between ultramafic rock and fractionating basaltic magma, I. Phase relations, the origin of calc-alkaline magma series, and formation of discordant dunite. Journal of Petrology, 31, 51-98.

Kelemen, P.B., Dick, H.J.B. and Quick, J.E. (1992) Formation of harzburgite by pervasive melt/rock reaction in the upper mantle. Nature, 358, 635-641.

Kong, P., Ebihara, M. and Palme, H. (1999) Siderophile elements in Martian meteorites and implications for core formation in Mars. Geochimica et Cosmochimica Acta, 63, 1865-1875.

Kring, D.A., Gleason, J.D., Swindle, T.D., Nishiizumi, K., Caffee, M.W., Hill, D.H., Jull, A.J.T. and Boynton, W.V. (2003) Composition of the first bulk melt sample from a volcanic region of Mars: Queen Alexandra Range 94201. Meteoritics & Planetary Science, 38, 1833-1848.

Kushiro, I. (1969) The system forsterite-diopside-silica with and without water at high pressures. American Journal of Science Schairer, 267-A, 269-294.

Longhi, J. (1995) Liquidus equilibria of some primary lunar and terrestrial melts in the garnet stability field. Geochimica et Cosmochimica Acta, 59, 2375-2386.

Longhi, J. and Pan, V. (1989) The parent magmas of the SNC meteorites. Procedings of the 19th Lunar and Planetary Science Conference, 451-464.

Longhi, J., Knittle, E., Holloway, J.R. and Wänke, H. (1992) The bulk composition, mineralogy, and internal structure of Mars. In Mars (Kieer, H.H. et al. Eds.). University of Arizona Press, Tucson, 184-208.

Matsukage, K.N. and Kubo, K. (2003) Chromian spinel during melting experiments of dry peridotite KLB-1) at 1.0-2.5GPa. American Mineralogist, 88, 1271-1278.

McCarthy, T.S., Erlank, A.J., Willis, J.P. and Ahrens, L.H. (1974) New chemical analyses of six achondrites and one chondrite. Meteoritics, 9, 215-221.

McCoy, T.J., Taylor, G.J., Keil, K. and Noll, P.D. (1991) Zagami: product of a two-stage magmatic history. Abstracts of the Lunar and Planetary Science Conference, 22, 867-868.

McKenzie, D., Jackson, J. and Priestley, K. (2005) Thermal structure of oceanic and continental lithosphere. Earth and Planetary Sciemce Letters, 233, 337-349.

McSween, H.Y. and Jarosewich, E. (1983) Petrogenesis of the Elephant Moraine A79001 meteorite: Multiple magma pulses

Advance Publication Article

on the shergotite parent body. Geochimica et Cosmochimica Aata, 47, 1501–1513.

McSween, H.Y., Arvidson, R.E., Bell, J.F., Blaney, D., Cabrol, N.A., Christ, P.R., Crisp, J.A., Crumpler, L.S., Des Marais, D.J., Farmer, J.D., Gellert, R., Ghosh, A., Grant, J., Haskin, L.A., Herkenhoff, K.E., Johnson, J.R., Jolliff, B.L., Klinge, G., McLennan, S., Milam, K.A., Moersch, J.E., Morris, R.V., Rieder, R., Ruff, S.W., Squyres, S.W., Wänke, H., Wang, A., Wyatt, M.B., Yen, A. and Zipfel, J. (2004) Basaltic rocks analyzed by the Spirit rover in Gusev Crater. Science, 305, 842–845.

McSween, H.Y., Wyatt, M.B., Gellert, R., Bell, J.F., Morris, R.V., Herkenhoff, K.E., Crumpler, L.S., Milam, K.A., Stockstill, K.R., Tornabene, L.L., Arvidson, R.E., Bartlett, P., Blaney, D., Cabrol, N.A., Christensen, P.R., Clark, B.C., Crisp, J.A., Des Marais, D.J., Economou, T., Farmer, J.D., Farrand, W., Ghosh, A., Golombek, M., Gorevan, S., Greeley, R., Hamilton, V.E., Johnson, J.R., Joliff, B.L., Klingelhöfer, G., Knudson, A.T., McLennan, S., Ming, D., Moersch, J.E., Rieder, R., Ruff, S.W., Schröder, C., de Souza, P.A., Squyres, S.W., Wänke, H., Wang, A., Yen, A. and Zipfel, J. (2006) Characterization and petrologic interpretation of olivine-rich basalts at Gusev Crater, Mars. Journal of Geophysical Research, 111, doi:10.1029/2005JE002477.

Meyer, C. (2003) Mars meteorite compendium 2003, http://curator.jsc.nasa.gov/antmet/mmc/mmc.htm

Minitti, M.E., Fei, Y. and Bertka, C.M. (2006) New, geophysically-constrained martian mantle compositions. Workshop on Earth and Planetary Differentiation, 72–73.

Misawa, K. (2004) The Yamato980459 olivine-phyric shergottite consortium. Antarctic Meteorite Research, 17, 1–12.

Monders, A.G., Medard, E. and Grove, T.L. (2007) Phase equilibrium investigations of the Adirondack class basalts from the Gusev plains, Gusev crater, Mars. Meteoritics & Planetary Science, 42, 131–148.

Musselwhite, D.S., Dalton, H.A., Kiefer, W.S. and Treiman, A.H. (2006) Experimental petrology of the basaltic shergottite Yamato-980459: Implications for the thermal structure of the Martian mantle. Meteoritics & Planetary Science, 41, 1271–1290.

Pepin, R.O. (1985) Meteorites: Evidence of Martian origins. Nature, 317, 473–475.

Quick, J.E. (1981) The origin and significance of large, tabular dunite bodies in the Trinity peridotite, northern California. Contributions to Mineralogy and Petrology, 78, 413–422.

Peslier, A.H., Hnatyshin, D., Herd, C.D.K., Walton, E.L., Brandon, A.D., Lapen, T.J. and Shafer, J.T. (2010) Crystallization, melt inclusion, and redox history of a Martian meteolite: Olivine-phyric shergottite Larkman Nunatak 06319. Geochimica et Cosmochimica Acta, 74, 4543–4576.

Righter, K., Yang, H., Costin, G. and Downs, R.T. (2008) Oxygen fugacity in the Martian mantle controlled by carbon: New constraints from the nakhlite MIL03346. Meteoritics & Planetary Science, 43, 1709–1723.

Ringwood, A.E. (1966) The chemical composition and origin of the Earth. In Advances in Earth Sciences (Hurley, P.M. Ed.). MIT Press, Cambridge, Mass., 287–356.

Rubin, A.E., Warren, P.H., Greenwood, J.P., Verish, R.S., Leshin, L.A., Hervig, R.L., Clayton, R.N. and Mayeda, T.K. (2000) Los Angeles: The most differentiated basaltic martian meteorite. Geology, 28, 1011–1014.

Sarbadhikari, A.B, Day, J.M.D., Liu, Y., Rumble, D. and Taylor, L.A. (2009) Petrogenesis of olivine-phyric shergottite Larkman Nunatak 06319: Implications for enriched components in martian basalts. Geochimica et Cosmochimica Acta, 73, 2190–2214.

Schilling, J.G., Zajac, M., Evans, R., Johnston, T., White, W., Devine, J.D. and Kingsley, R. (1983) Petrologic and geochemical variations along the Mid-Atlantic Ridge from 29 degrees N to 73 degrees N. American Journal of Science, 283, 510–586.

Shearer, C.K., Burger, P.V., Papdce, J.J., Borg, L.E., Irving, A.J. and Herd, C. (2008) Petrogenetic linkages among Martian basalts: Implications based on trace element chemistry of olivine. Meteoritics & Planetary Science, 43, 1241–1258.

Shih, C.Y., Nyquist, L.E., Wiesmann, H., Reese, Y. and Misawa, K. (2005) Rb-Sr and Sm-Nd dating of olivine-phyric shergottite Yamato 980459: Petrogenesis of depleted shergottites. Antarctic Meteorite Research, 18, 46–65.

Stolper, E. and McSween, H.Y. (1979) Petrology and origin of the shergottite meteorites. Geochimica et Cosmochimica Acta, 43, 1475–1498.

Takahashi, E., Shimazaki, T., Tsuzaki, Y. and Yoshida, H. (1993) Melting study of a peridotite KLB-1 to 6.5 GPa and the origin of basaltic magmas. Philosophical Transactionof Royal Society of London, A 342, 105–120.

Taylor, L.A., Nazarov, M.A., Shearer, C.K., McSween, H.Y., Cahill, J., Neal, C.R., Ivanova, M.A., Barsukova, L.D., Lentz, R.C., Clayton, R.N. and Mayeda, T.K. (2002) Martian meteorite Dhofar019: A new shergottite. Meteoritics & Planetary Science, 37, 1107–1128.

Usui, T., McSween, H.Y. and Floss, C.(2008) Petrogenesis of olivine-phyric shergottite Yamato 980459, revisited. Geochimica et Cosmochimica Acta, 72, 1711–1730.

Wadhwa, M., Lentz, R.C.F., McSween, H.Y. and Crozaz, G. (2001) A petrologic and trace element study of Dar al Gani 476 and Dar al Gani 489: Twin meteorites with affinities to basaltic and lherzolitic shergottite. Meteoritics & Planetary Science, 36, 195–208.

Walter, M.J. (1998) Melting of garnet peridotite and the origin of komatiite and depleted lithsphere. Journal of Petrology, 39, 29–60.

Warren, P.H., Kallemeyn, G.W. and Kyte, F.T. (1999) Origin of planetary cores: evidence from highly siderophile elements in martian meteorites. Geochimica et Cosmochimica Acta, 63, 2105–2122.

Yoder, C.F., Konopliv, A.S., Yuan, D.N., Standish, E.M. and Folker, W.M. (2003) Fluid core size of Mars from detection of the solar tide. Science, 300, 299–303.

Zipfel, J., Scherer, P., Spettel, B., Dreibus, G. and Schultz, L. (2000) Petrology and chemistry of the new shergottite Dar al Gani 476. Meteoritics & Planetary Science, 35, 95–106.

Manuscript received August, 20, 2012
Manuscript accepted February, 28, 2013

Manuscript handled by Eiji Ohtani

Advance Publication